The Role of Wall Shear Stress in Unsteady Vascular Dynamics

M. GRIGIONI, C. DANIELE, G. D'AVENIO
Laboratory of Biomedical Engineering, Istituto Superiore di Sanità, Rome, Italy

G. PONTRELLI
Istituto per le Applicazioni del Calcolo – CNR, Rome, Italy

Summary

The role of the pulsatile wall shear stress in blood flow is shown by an in vivo experiment. Measures of wall shear rate and other hemodynamic variables are provided and allow for the possible comparison with other experiments. Then, the complex rheological properties of the blood are taken into account by means of a non-Newtonian model applied to a simpler flow. Numerical simulations and results of experiments show the effect of the wall mechanics and of the fluid material nonlinearities on the hemodynamics. The evaluation of wall shear stress is discussed and some potential clinical implications are outlined.

Key Words

Viscoelasticity, shear-thinning fluids, blood flow, numerical methods

Introduction

Both mathematical and experimental models are widely used for describing unsteady blood flows and for understanding typical features in vascular dynamics. Because of the importance of hemodynamic factors, and in particular of the wall shear stress (WSS), in the development of arterial pathologies, many experimental and theoretical studies have been carried out. Recently, WSS has been correlated with atherosclerosis; Krams et al. [1] established a reciprocal relationship between wall thickness and mean WSS. Moreover, there is some evidence that hemodynamic anomalies are related to transient flows, and that the alteration of the WSS depends on the variation of some other physical variables.

Generally, determining WSS is a difficult task for both in vivo and in vitro experiments. In vivo studies are complicated by the unsteadiness of the flow modulated by respiration, as well as by the resolution features of the clinical apparatus. A number of investigators have used several techniques (ultrasound [2], nuclear magnetic resonace [3], and Laser Doppler anemometry [4]) to estimate WSS on the basis of velocity data. However, the rigorous evaluation of WSS would require the precise measurement of the blood's rheological properties. On the other hand, in vitro experiments exhibit a low representativity due to the unrealistic conditions and the use of blood-analogous fluids. While some researchers have emphasized the importance of the mean value of the WSS in the process of vascular remodeling, others such as Delfino et al. [5] and Lee and Tarbell [6] have stressed the importance of the oscillating WSS. The role of WSS in the onset of smooth muscle cell proliferation has also been recognized in vivo, using an animal model of a vascular prosthesis implantation. In fact, intimal thickening represents an important clinical problem in atherosclerosis and in the design of vascular grafts employed to bypass diseased arteries. Kraiss et al. [7] found that the neointimal cross-sectional area in high shear stress grafts was substantially lower than in the low shear stress grafts. A number of studies have suggested relationships between various measures of WSS and intimal thickening in the affected vessels [8]. Further experimental results have shown alterations in the blood's biochemical structure. For example, in a model of stenosed coronary arteries, Holme et al. found that high WSS was correlated with platelet activation and

platelet micro-particle formation [9]. In the present study, the role of WSS is highlighted by an in vivo experiment performed on the carotid artery [10]. Results of such an investigation have to be assessed and can be used as an evaluation tool for numerical simulations. Actually, many mathematical models for describing rheological behavior of blood have been extensively developed, but a universally accepted theoretical model of the mechanics of continuum is still lacking (see [11] for a recent review). Although it has been well established that blood is both a viscoelastic and a shear-thinning liquid, the connection between these two characteristics has not yet been clarified [12]. Due to the highly nonlinear behavior of these non-Newtonian models, some appropriate simplified methods to study the flow are necessary. The first step in studying the mechanics of circulation is the investigation of flows in straight uniform tubes; any spurious effect due to the geometry is thus removed. Some numerical results of a non-Newtonian model used for simulating blood in typical unsteady flows will be reported [13,14]. They concern flows in a rigid tube driven by some known pressure gradients. Although these flows are unrealistic in describing the real blood circulation, they nevertheless offer a useful tool for setting up the model and for understanding the main characteristics of pulsatile flows, since any pressure pulse can be regarded as a superposition of oscillations.

The coupled constitutive and motion equations form a nonlinear system which is numerically solved with a spectral collocation method in space and a finite difference method in time. The flow dependence on the physical parameters in connection with the unsteadiness is investigated carefully and the presence of normal stress is outlined.

Materials and Methods

In-Vivo Experiment

Many theories have established a correlation between some hemodynamic variables and the intimal thickening of the vessel walls. To confirm this relationship, a particular vascular environment has been imposed by means of the Moncada experimental model [10]. This technique consists of detaching an arterial segment from the surrounding tissues, without impairment to the structure that supplies blood to the vessel itself, so that only the mechanical aspects are altered and possible ischemic effects are excluded. Subsequently, a non-constrictive plastic collar is placed around the artery, which is thus left free to expand within it. As a consequence, with the perivascular tethering excluded, the biomechanics of the wall and the fluid dynamics are altered without any endothelium damage. This procedure has been applied to New Zealand rabbits whose carotid arteries measure about 2 – 3 mm in diameter. The evolution of the hemodynamics of the manipulated vessel has been monitored with a 0.3 mm spacing between the consecutive points, by means of a pulsed real-time Ultrasound Doppler profilometer (DOP1000, Signal Processing S.A., Switzerland), with a transmission frequency of 8 MHz. This occurred several days after implantation of the collar that was used to isolate the artery. The experiments have been made in compliance with the recommendations of the Council of the European Community (86/609/EEC). Software has been developed to approximate the radius dependency of the velocity in the pipe's direction with the following function:

$$w(r) = W_{Max}\left[1-\left(\frac{r}{R}\right)^{\alpha}\right] \qquad \alpha \geq 0,\ R > 0 \qquad (1.1)$$

This generalizes the Poiseuille flow. Each velocity profile has been reconstructed by the best fit (in the least square sense) of the recorded data with respect to α and R. We used all the validated velocity points along the vessel's lumen, not just those lying closer to the vessel's wall. These are usually affected by a low signal-to-noise ratio and are possibly corrupted by reflections originated at the vessel-blood interface. An alternative approach has been used when a region of flow reversal was occasionally detected; in this case, the software automatically reconstructs the velocity profile by using a cubic spline interpolating all of the measured points. The two halves of the flow profile, proximal and distal to the transducer, have been reconstructed independently and averaged over 3 cycles. Because of the possible influence of the respiratory rhythm in determining a modulation of the recorded profile, the averaging procedure has been made on data relative to the same respiratory phase. The values of the wall shear rate (WSR) and centerline velocity are relative to the highest systolic peaks.

Since rigorous evaluation of the WSS would require precise measurement of the blood's rheological properties (see next section), measurements of the wall shear rate (WSR) are provided. Although the WSR is a less

physically significant parameter than the WSS, the WSR is more easily measurable and enables a direct comparison with other experiments. By assuming that the radial component of velocity is negligible, WSR values are easily computed by evaluating the *r*-derivative of *w* at the wall [12]:

$$\dot{\gamma}_R = -\left.\frac{dw}{dr}\right|_{r=R} = W_{Max}\frac{\alpha}{R} \qquad (2.1)$$

The magnitude of the WSR depends on the arterial site: deviations from standard values are indicative of pathologic states; for example, the value of 420 s^{-1} is found in healthy, small, coronary arteries, whereas values of 2600 – 15000 s^{-1} are found in vessels with various degrees of stenotic lesions [15].

Shear-Thinning Viscoelastic Model for Blood Flow

Mathematical models of blood flow constitute an alternative and useful tool for supporting experiments and detect minor phenomena and local features which are not obvious by measurements. For example, non-Newtonian models introduce the effect of a non-constant viscosity, by considering the rheological behavior of blood. The linear theory of Navier-Stokes fluid is widely used for modeling blood flow in large arteries, but the role of material nonlinearity and the influence of red cells on the viscosity become more important at low shear rates (< 100 s^{-1}) as well as in smaller vessels, where flows cannot be well described by a simplistic linear constitutive equation [16].

In the microcirculation, both the Reynolds and Womersley numbers are small because of the small size of the vessels and the low flow velocities. Moreover, near the center of the large vessels, or in separated regions of recirculating flow, the mean value of shear rate $\dot{\gamma}$ will be small and, in unsteady flows, may disappear in some instances. In all these cases, the viscosity μ cannot be considered as a constant, but as a decreasing function of the shear rate $\dot{\gamma}$ (shear-thinning fluid). In the early 1990s, many functions were proposed for modeling the nonlinear dependence of the viscosity of the blood on the strain rate [17,18]. Due to the variable behavior and the complex chemical structure of this liquid, none of the models seem to be completely satisfactory for all kinds of flow regimens.

General regression analysis of experimental data suggests the use of some complicated transcendental functions for $\mu(\dot{\gamma})$. Since the apparent viscosity has two distinct asymptotic values η_0 and η_∞ as $\dot{\gamma} \to 0$ and $\dot{\gamma} \to \infty$ respectively ($\eta_0 \geq \eta_\infty$), the analytical function which offers the best fit for experimental data with a large range of flows has been found to be:

$$\mu(\dot{\gamma}) = \eta_\infty + (\eta_0 - \eta_\infty)\left[\frac{1+\log(1+\Lambda\dot{\gamma})}{1+\Lambda\dot{\gamma}}\right]$$

$$\dot{\gamma} = \left[\frac{1}{2}\mathrm{tr}\boldsymbol{A}_1^{\,2}\right]^{1/2} \qquad \boldsymbol{A} = \boldsymbol{L} + \boldsymbol{L}^T, \quad \boldsymbol{L} = \nabla\boldsymbol{v} \qquad (3.1)$$

with $\Lambda \geq 0$ a material constant with the dimension of time, representing the degree of shear-thinning [19]. The complex viscosity of blood is approximated here with a three-parameter model, where the apparent viscosity decreases dramatically as the rate of shear increases. The asymptotic values η_0 and η_∞ are present in many other inelastic shear-thinning models and their values have been set up through experiments. A pure inelastic model based on the equation (3.1) captures some aspects of the shear-thinning, but does not address any shear history dependence, and it is insufficient to correctly describe the unsteady blood flow. Experimental results show that blood is not a purely viscous fluid, but possesses significant viscoelastic properties [12,16]. A time lag in the response of the fluid to changes in loading forces is observed and rate type models are commonly used to describe such strain and stress history dependence.

The relationship between the extra-stress tensor $\boldsymbol{S}$ and the stretching tensor $\boldsymbol{A}_1$ in the well known viscoelastic Oldroyd-B fluid [17] can be easily generalized by considering the function $\mu(\dot{\gamma})$ defined in (3.1), instead of a constant viscosity μ, as follows:

$$\boldsymbol{S} + \lambda_1\left(\dot{\boldsymbol{S}} - \boldsymbol{L}\boldsymbol{S} - \boldsymbol{S}\boldsymbol{L}^T\right) = \mu(\dot{\gamma})\boldsymbol{A}_1 + \eta_0\lambda_2\left(\dot{\boldsymbol{A}}_1 - \boldsymbol{L}\boldsymbol{A}_1 - \boldsymbol{A}_1\boldsymbol{L}^T\right) \qquad (3.2)$$

where λ_1 and λ_2 are two constants, having the dimension of time ($\lambda_1 \geq \lambda_2 \geq 0$), referred to as relaxation and retardation time, respectively; the dot over a variable f, which might be a scalar, vector, or tensor, denotes the material derivative as in: $\dot{f} = \partial f/\partial t + \boldsymbol{v}\cdot\nabla f$. Equation (3.2), by combining elastic and viscous terms, can be used to predict, at least qualitatively, many of the properties observed in blood flows. The model (3.2) reduces to a pure inelastic fluid when $\lambda_1 = \lambda_2 = 0$ and to

the Navier-Stokes linear model when, in addition, $m(\dot{g})$ const (i.e., $\eta_0 = \eta_\infty$).

A Mathematical Model for an Unsteady Flow in a Rigid Pipe

As a benchmark for measuring the capabilities of the model (3.2), some unsteady flows in a cylindrical long pipe (i.e., of length much larger than the radius of the pipe) with a circular cross section having the radius R have been studied. The fluid is assumed to be an isotropic, homogeneous and incompressible continuum of constant density ρ, and the vessel walls are considered rigid and impermeable. The motion equation is:

$$\rho \frac{\partial \mathbf{v}}{\partial t} + \mathbf{v} \cdot \nabla \mathbf{v} = \nabla \cdot \mathbf{T} \tag{4.1}$$

where $\mathbf{T} = -p\mathbf{I} + \mathbf{S}$ is the stress tensor, $\mathbf{v} = (u, v, w)$ is the velocity vector and the external forces are supposed negligible. Let us now consider a cylindrical coordinate system (r, θ, z) , where the z axis coincides with the pipe axis. In the hypothesis of laminar flow, the only non-zero component of velocity is w. Moreover, since the flow is assumed to be axisymmetric and with no entry effect, the fluid dynamic variables do depend on r and t only, except for the pressure, which depends on z and t only. The flow is driven by the following oscillatory pressure gradient: $\partial p/\partial z = A\cos(\omega t)$ for $0 \le t \le T$. The constitutive equation (3.2), with the expression of viscosity (3.1), coupled with the motion equation (4.1), gives:

$$\rho \frac{\partial w}{\partial t} = -\frac{\partial p}{\partial z} + \frac{\partial S_{rz}}{\partial r} + \frac{S_{rz}}{r}$$

$$S_{rz} + \lambda_1 \frac{\partial S_{rz}}{\partial t} = \left[\eta_\infty + (\eta_0 - \eta_\infty)\frac{1+\log\sigma}{\sigma}\right]\frac{\partial w}{\partial r} + \eta_0 \lambda_2 \frac{\partial^2 w}{\partial r \partial t}$$

$$S_{zz} + \lambda_1\left(\frac{S_{zz}}{\partial t} - 2\frac{\partial w}{\partial r}S_{rz}\right) = -2\eta_0\lambda_2\left(\frac{\partial w}{\partial r}\right)^2 \tag{4.2}$$

where $\sigma = 1 + \Lambda\left|\frac{\partial w}{\partial r}\right|$

Note that in case of a pure shear-thinning fluid ($\lambda_1 = \lambda_2 = 0$), we have:

$$S_{rz} = \left[\eta_\infty + (\eta_0 - \eta_\infty)\frac{1+\log\sigma}{\sigma}\right]\frac{\partial w}{\partial r}$$
$$S_{zz} = 0 \tag{4.3}$$

The expression (4.3) can be used to compute S_{rz} at the wall (WSS), once the value of $dw/dr|_{r=R}$ is derived from the experiments. The boundary conditions associated with the physical problem are given by: $w = 0$ at $r = R$ (no slip velocity at the wall) and $dw/dr = 0$ at $r = 0$ (axisymmetry) and an initial condition is assigned. The complexity and the nonlinearity of the problem requires a careful numerical treatment. The first and second equation (4.2), after nondimensionalization, are rewritten as:

$$\frac{\partial \phi}{\partial t} = G(\phi) + f(t) \tag{4.4}$$

where $\phi = (w, S_{rz})$ and G is the nonlinear differential operator for spatial terms and f is the forcing term. Then, the partial differential equations (4.4) are split into two subsequent differential problems consisting first in discretizing the spatial operator G with an accurate and efficient method, and in integrating a system of ordinary differential equations in time with the implicit second order trapezoidal scheme (method of the lines or semidiscretization). Due to the stronger dependence on the space variables, the higher order, and the nonlinearities, a spectral collocation method has been used to approximate the spatial operator G [20]. With G being the nonlinear operator, we solved the discretized form of (4.4) by linearized iterations at each time step, computing the viscosity coefficient [$\eta_\infty + (\eta_0 - \eta_\infty)(1 + \log \sigma)/\sigma$] explicitly. The iteration proceeds until convergence is reached. Then, a value for S_{zz} is obtained explicitly by discretizing the third equation (4.2) in time. The coefficients of the spectral representation are computed at each time step as a solution of the algebraic linear system. This is the major time-consuming step in the integration procedure, because of the iteration loop within each time step. For further computational details see Pontrelli [13]. Other aspects of such non-Newtonian models have been investigated for a flow driven by an impulsive pressure gradient [14], and for the blood flow of the shear-thinning fluid (3.1) through an axisymmetric stenosis [21].

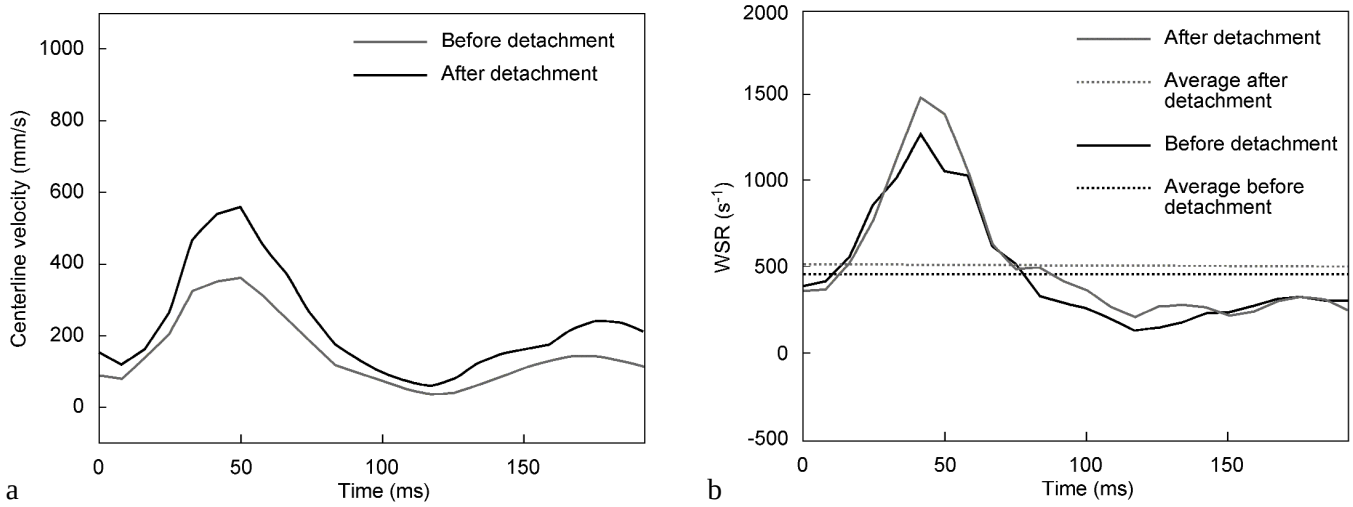

Figure 1. Comparison of hemodynamic variables before and after detachment of muscle planes: centerline velocity (panel a) and wall shear stress (panel b). Horizontal lines (panel b) refer to mean wall shear stress (WSR).

	Collar implantation	1 day after collar implantation	7 days after collar implantation	14 days after collar implantation
Mean WSR (s^{-1})	1432 ± 137	1831 ± 106	2347 ± 99	2432 ± 143
Peak to peak WSR (s^{-1})	1654 ± 241	2551 ± 235	2875 ± 826	3113 ± 253
Peak centerline velocity (mm/s)	720 ± 89	983 ± 158	913 ± 131	969 ± 113

Table 1. Fluid dynamic variables after collar implantation.

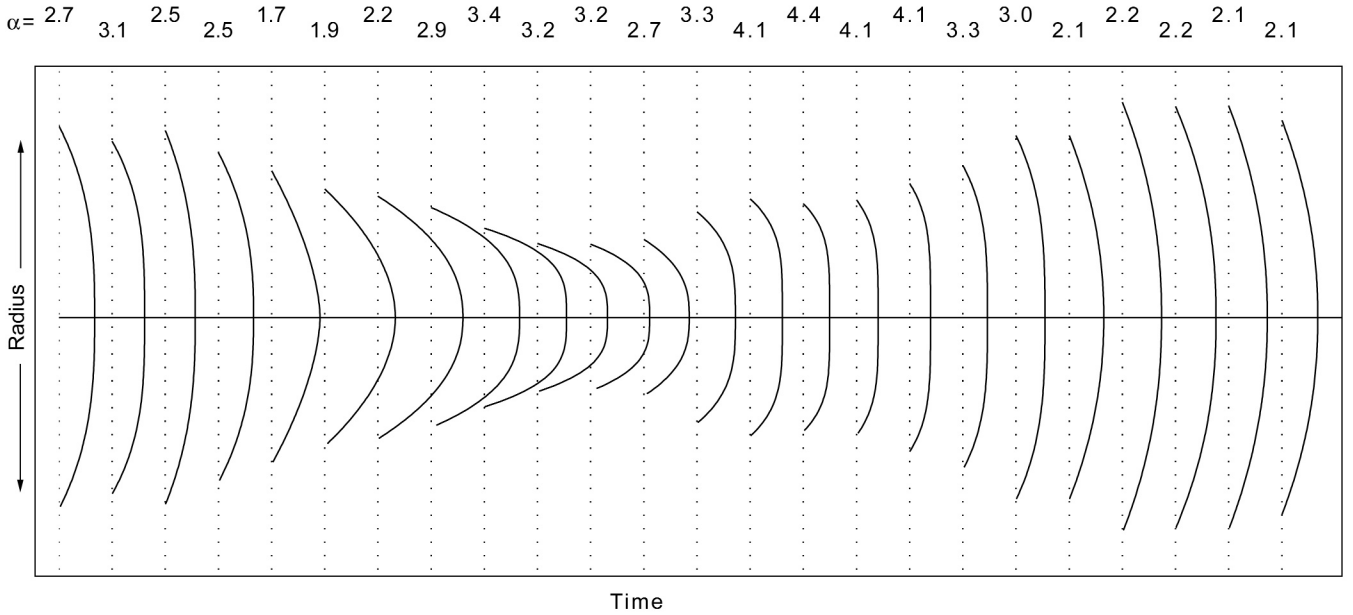

Figure 2. Computed velocity profiles along one cycle (1 day after collar implantation) with the value of a obtained by fitting equation (1.1) to the axial velocity profile.

Results and Discussion

In-vivo Experiment

The main effect of the perivascular manipulation on hemodynamics is the increase of the mean and of the oscillating WSR, as well as of the centerline velocity peak values, even a few moments after vessel isolation (Fig. 1). Although the mean WSR values do not increase considerably during the first days of collar implantation, a progressive rise is reported in the following days (see Table 1). This fact is deemed responsible for the decreasing rate of cellular proliferation [1]. Figure 2 shows the evolution of the computed velocity profiles, in a condition (one day after collar placement) characterized by enhanced oscillations. In the acceleration phase, the flow tends to be a flat profile in the core (plug flow), and is satisfactorily described by the function (2.1), with $a \geq 2$ (Reynolds number ≈ 600). The bluntness index α is increasingly found as the flow approaches the systolic peak, as well as in the subsequent deceleration phase. Measurements over several series of 6 samples showed a high correlation between the oscillation of WSR and the intimal thickening during the time of the experiment. The correlation coefficient was found to be 0.95 (significant level: p-value < 0.05) [2].

In-Vivo Experiment

The findings from the in-vivo experiment suggest that the onset of the intimal hyperplasia is related to the increased WSR oscillations consequent to the modified wall mechanics. This fact should be carefully considered in the pharmacological treatment of atherosclerosis because vasoactive substances can be successfully employed to investigate the possibility of inhibiting the disease progress as shown in [15].

Numerical Simulation

The numerical results of the model for an unsteady flow in a rigid pipe are not directly related to the above in-vivo experiment; nevertheless, as a prototype, they offer a clear indication of the importance of shear rate dependent viscosity and of the fluid viscoelasticity. They also provide an easy and accurate computation of the hemodynamic variables, once the material parameters are adjusted. This is of some relevance in the localization of vascular diseases and in clinical procedures, such as vascular wall remodeling or design of artificial prostheses. For example, the magnitude and the variation of the WSS are relevant clues for the localization

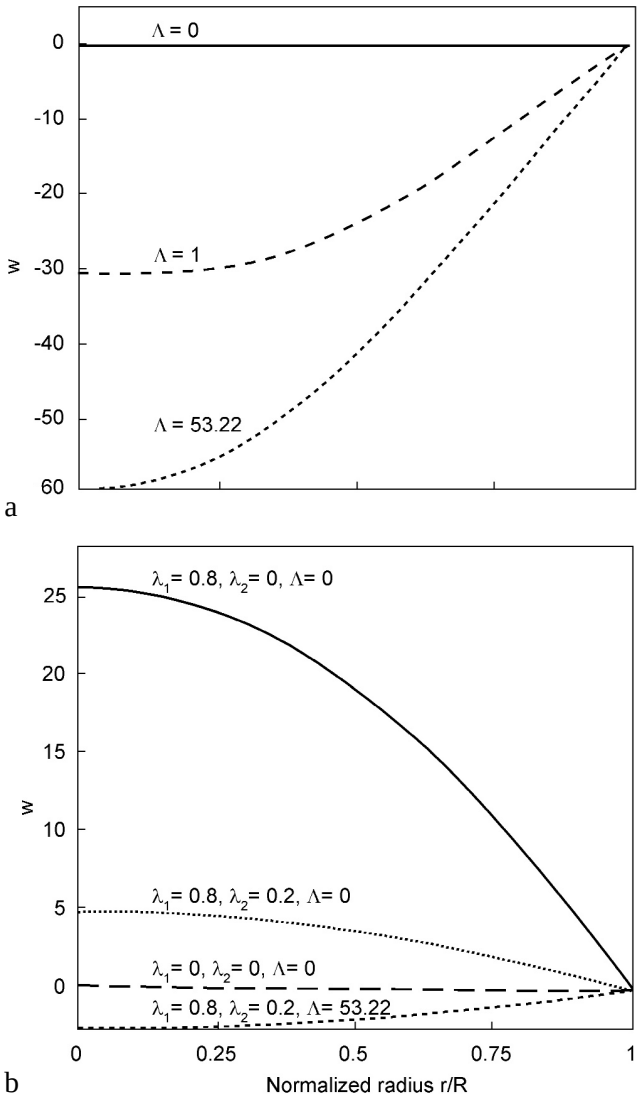

Figure 3. Nondimensional profiles of the axial velocity profiles w at 3/4 period for the non-Newtonian model of equations (3.1) in panel a) and (3.2) in panel b) for different parameters.

and prediction of diseases in blood vessels. It has been shown that if the WSS reaches a value higher than 400 dyne/cm^2 the endothelial surface is irreversibly damaged, and this might be a factor in atherogenesis [11]. Since we restrict ourselves to the flow in small vessels, the parameters have been adjusted to some extent to the blood flow; some of them are typical of physiologic measurements and are chosen to obtain a velocity waveform with characteristics similar to the artery velocity pulses [12]:

$\rho = 1.05$ g cm^{-3}, $\eta_0 = 180$ *cP*, $\eta_\infty = 3.96$ *cP*,
$A = 2600$ cm s^{-2}, $\omega = 8$ s^{-1}, $R = 0.1$ cm.

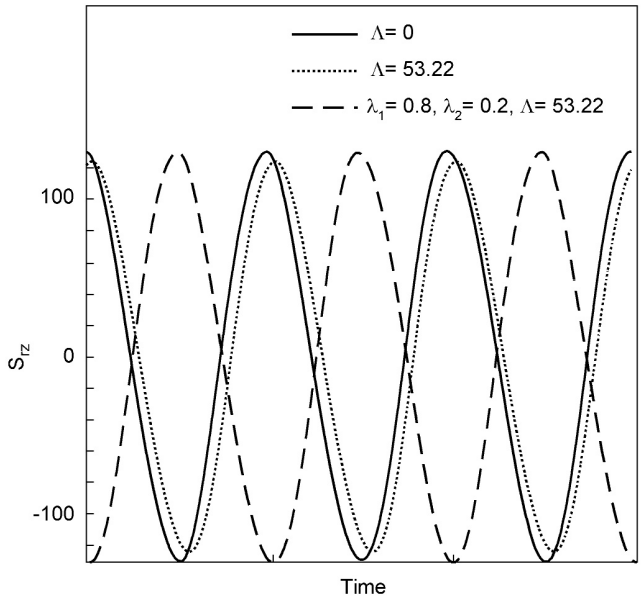

Figure 4. Evolution of the nondimensional wall shear stress (WSS) at the wall $S_{rz}|_{r=R}$ over three periods for the non-Newtonian model of equations (3.1) and (3.2) for different values of the parameters.

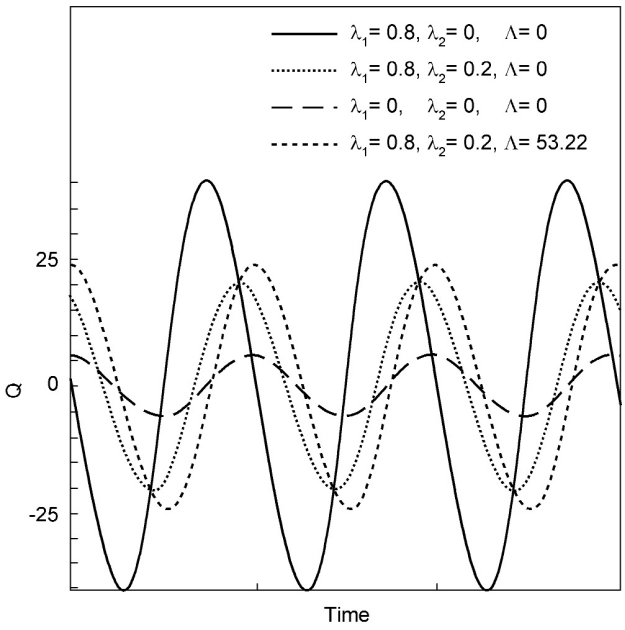

Figure 5. Evolution of nondimensional flow rate Q, which is found by integrating the axial velocity w across the tube cross-section, over three periods for the non-Newtonian model of equations (3.1) and (3.2) for different parameters.

The other parameters are varied in a typical range to test the sensitivity of the system to their perturbation. Simulations have been carried out with $\Delta t = 10^{-4}$, and the degree of approximating polynomials (and of the number of approximating points) is chosen as n = 20. The numerical solution obtained with the setting $l_1 = l_2 = L = 0$ is compared with the exact solution in the case of a Navier-Stokes fluid, to give some estimate as to the accuracy and stability of the numerical method. The fine agreement obtained ($\|e\|_\infty \leq 10^{-5}$) confirms the effectiveness of the scheme used.

To evaluate the importance of the concurrent viscous and elastic forces and to understand the role of each of them, the special cases $l_1 = l_2 = 0$ (pure shear-thinning fluid) and $L = 0$ (pure Oldroyd-B fluid) are considered separately. In the pure shear-thinning fluid there is a considerable increase of velocity with L at any time. Also, the variation of l_1 and l_2 increases the velocity (but with a different order of magnitude or different sign), and when the three parameters are changed at the same time, the profile may appear reversed. Sometimes the shear-thinning effect amplifies that of the viscoelasticity, other times it hinders it (Figure 3); the time history of WSS in the last three cycles is plotted in Figure 4. Despite an increased value of the velocity, a slight reduction in amplitude and a phase shift of WSS in the case $L \neq 0$ is obtained.

On the other hand, WSS exhibited in viscoelastic cases has a phase lead ($\cong 180°$) over that found in the inelastic cases, but its magnitude stays under the critical

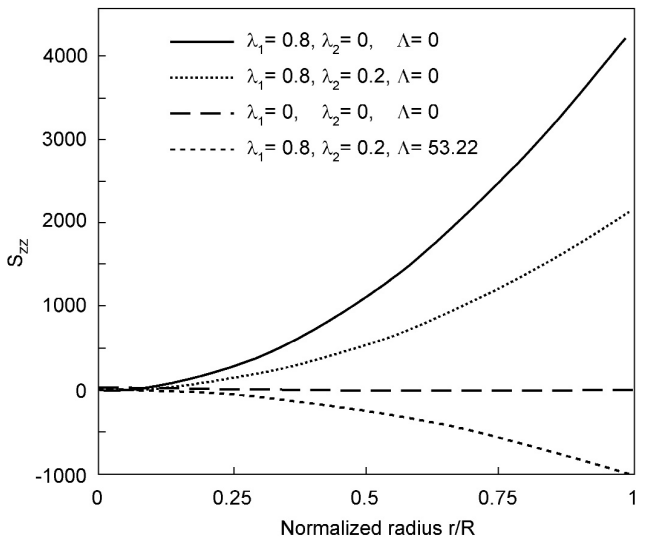

Figure 6. Nondimensional normal stress $S_{zz}|_{r=R}$ at 3/4 period for the non-Newtonian model of equations (3.1) and (3.2) for different values of the parameters.

value for all times. Estimates of WSS (by considering previous WSR values in experiments) are derived both in the Newtonian and in pure shear-thinning cases according to equation (4.3). The maximum relative difference along one cardiac cycle was found to be less than 4%. This is because the magnitude of WSR is relatively high and the non-Newtonian character of the fluid has a limited influence. In Figure 5 the evolution of the flow rate is shown for some values of the parameters. An increase of L only causes a noticeable rise of the amplitude, while both amplitude and phase change along l_1, l_2, and L. Other physical phenomena have some clinical implications: due to the fact that the viscosity is confined in a thin layer near the wall, the effect of unsteadiness is more evident at the center, because this region responds more promptly to variations in the driving pressure gradient. Phenomena of backflow can be present. While in a pure shear-thinning fluid $S_{zz} = 0$, in the other cases the normal stress S_{zz} is not zero, and can reach an order of magnitude larger than the shear stress; it is most sensitive to the variation of parameters (Figure 6).

Conclusion

Vessel wall remodeling is the supposed mechanism involved in important vascular diseases (atherosclerosis, intimal hyperplasia, and restenosis), as an adaptive response to the pathologic states of arteries. The role of the unsteady WSS and of other hemodynamic variables has been established on an experimental basis. Results have shown that the intimal thickening is correlated with the pulsatile WSS and, in general, with the biomechanics of the wall. This is in agreement with other research, which suggests that the flow-derived mechanical stress induces modifications at the wall level. Therefore, an accurate description of the magnitude and variation of the WSS is useful for detecting the early stages of vascular lesions.

The use of a mathematical model which combines the action of the viscoelasticity and shear-rate dependent viscosity supports and complements the presented experiment. It allows us to understand the importance of the rheology in blood flow, at least from a qualitative point of view. Although this preliminary study is restricted to a straight and rigid arterial segment, it offers the basis for a better understanding of blood flow in small vessels, provides hints on the physical phenomena occurring in more complex flows, and constitutes a first step in the development of further experiments. It has been established that a pure inelastic model is not representative of the rheological behavior of blood, but it cannot a priori be neglected. A more important role for WSS is played by the fluid viscoelasticity in time-dependent flows. The combination between a viscoelastic and a shear-thinning fluid induces effects that may not be present in each of them individually. All of these mechanical and biochemical aspects related to fluid dynamics are of some importance and demand further investigation. A great deal of work is needed to establish the rheological parameters for the physiologic values, and to understand the connection of these issues with the biological and clinical facts.

Acknowledgment

This work has been partially supported by the strategic project of the Italian National Council of Research, Methods and Models for the Study of Biological Phenomena, Italy, 2000 (Consiglio Nazionale delle Ricerche, CNR, Progetto Strategico, Metodi e Modelli Matematici nello studio di fenomeni biologici).

References

[1] Krams R, Wentzel JJ, Oomen JA, et al. Shear stress in arteriosclerosis, and vascular remodelling. Semin Interv Cardiol. 1998; 3: 39-44.

[2] Grigioni M, Marano G, Formigari R, et al. Wall shear stress swing and the development of intimal hyperplasia in rabbit carotid artery (abstract). In Proceedings of the XXV European Society for Artificial Organs ESAO Congress, 1998 Nov 11-13; Bologna, Italy. Int J Artif Organs. 1998; 21: 619.

[3] Oyre S, Ringgard S, Erlandsen M, et al. Automatic Accurate In Vivo Determinations of Blood Flow, Wall Shear Stress and Subpixel Vessel Wall Position in the Common Carotid Artery Throughout the Entire Heart Cycle by MRI (abstract). In 70th Scientific Sessions of the American Heart Association; 1997 Nov 10-14; Orlando, USA. Circulation. 1997; 96 (8 Suppl): I-50.

[4] Liepsch D, Pflugbeil G, Matsuo T, et al. Flow visualization and 1- and 3-D laser- Doppler-anemometer measurements in models of human carotid arterie. Clin Hemorheol Microcirc. 1998; 18: 1-30.

[5] Delfino A, Stergiopulos N, Moore JE Jr, et al. Residual strain effects on the stress field in a thick wall finite element model of the human carotid bifurcation. J Biomech. 1997; 30: 777-786.

[6] Lee CS, Tarbell JM. Influence of vasoactive drugs on wall shear stress distribution in the abdominal aortic bifurcation: an in vitro study. Ann Biomed Eng. 1998; 26: 200-212.

[7] Kraiss LW, Kirkman TR, Kohler TR, et al. Shear stress regulates smooth muscle proliferation and neointimal thickening in porous polytetrafluoroethylene graft. Arterioscler Thromb. 1991; 11: 1844-1852.

[8] Friedman MH, Deters O, Bargeron C, et al. Shear-dependent thickening of the human arterial intima. Arteriosclerosis. 1998; 9: 511-522.

[9] Holme PA, Orvim U, Hamers MJ, et al. Shear-induced platelet activation and platelet microparticle formation at blood flow conditions as in arteries with a severe stenosis. Arterioscler Thromb Vasc Biol. 1997; 17: 646-653.

[10] Yong AC, Townley G, Boyd GW. Haemodynamic changes in the Moncada model of atherosclerosis. Clin Exp Pharm & Physiol. 1992; 19: 339-342.

[11] Ku DN. Blood flow in arteries. Ann Rev Fluid Mech. 1997; 29: 399-434.

[12] Fung YC. Biomechanics. Circulation. New York: Springer. 1984.

[13] Pontrelli G. Pulsatile blood flow in a pipe. Computers & Fluids. 1998; 27: 367-380.

[14] Pontrelli G. Blood flow through a circular pipe with an impulsive pressure gradient. Math Models Methods in Appl Sci. 2000; 10: 187-202.

[15] Marano G, Palazzesi S, Bernucci P, et al. ET(A)/ET(B) receptor antagonist bosentan inhibits neointimal development in collared carotid arteries of rabbits. Life Sci. 1998; 63: PL259-266.

[16] Chien S, Usami S, Skalak R. Blood flow in small tubes. In: Renkins E, Michel CC (editors). Handbook of Physiology, Section 2: The cardiovascular system, Volume IV, Parts 1 & 2: Microcirculation. Bethesda: American Physiology Society. 1984: 217-249.

[17] Chmiel H, Anadere I, Walitza E. The determination of blood viscoelasticity in clinical hemorheology. Biorheology. 1990; 27: 883-894.

[18] Mann DE, Tarbell JM. Flow of non-newtonian blood analog fluids in rigid curved and straight artery models. Biorheology. 1990; 27: 711-733.

[19] Yeleswarapu KK. Evaluation of continuum models for characterizing the constitutive behavior of blood (dissertation). Pittsburgh: University of Pittsburgh. 1996.

[20] Canuto C, Hussaini MY, Quarteroni A, et al. Spectral method in Fluid Dynamics. Springer Series in Computational Physics. New York: Springer Verlag. 1987.

[21] Pontrelli G. Blood flow through an axisymmetric stenosis. Proc Inst Mech Eng, Part H, J Eng Med. 2001; 215: 1-10.

Contact
Dr. Mauro Grigioni
Laboratory of Biomedical Engineering
Istituto Superiore di Sanità
Viale Regina Elena 299
I-00161 Roma
Italy
Telephone: +39 06 4990 2855
Fax: +39 06 4938 7079
E-mail: grigioni@iss.it